ARTICLE

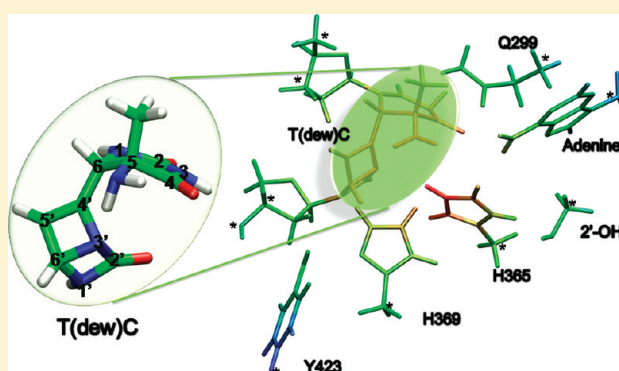# Repair of DNA Dewar Photoproduct to (6-4) Photoproduct in (6-4) Photolyase

Yue-Jie Ai,[†] Rong-Zhen Liao,[§] Shi-Lu Chen,[∥] Wei-Jie Hua,[†] Wei-Hai Fang,*[,‡] and Yi Luo*[,†]

[†]Theoretical Chemistry, School of Biotechnology, Royal Institute of Technology, SE-10691 Stockholm, Sweden

[‡]College of Chemistry, Beijing Normal University, Beijing 100875, People's Republic of China

[§]Department of Organic Chemistry, Arrhenius Laboratory, Stockholm University, SE-10691 Stockholm, Sweden

[∥]Key Laboratory of Cluster Science of Ministry of Education, School of Chemistry, Beijing Institute of Technology, Beijing 100081, People's Republic of China

S *Supporting Information*

ABSTRACT: Dewar photoproduct (Dewar PP) is the valence isomer of (6-4) photoproduct ((6-4)PP) in photodamaged DNA. Compared to the extensive studied CPD photoproducts, the underlying repair mechanisms for the (6-4)PP, and especially for the Dewar PP, are not well-established to date. In this paper, the repair mechanism of DNA Dewar photoproduct T(dew)C in (6-4) photolyase was elucidated using hybrid density functional theory. Our results showed that, during the repair process, the T(dew)C has to isomerize to T(6-4)C photolesion first via direct C6′−N3′ bond cleavage facilitated by electron injection. This isomerization mechanism is energetically much more efficient than other possible rearrangement pathways. The calculations provide a theoretical interpretation to recent experimental observations.

1. INTRODUCTION

With the increasing incidence of skin cancer, UV photo-damage of DNA has drawn considerable attention nowadays.[1,2] The absorption of the UV-light by DNA results in three reactive photochemical lesions. Compared to the two frequently found photoproducts, cyclobutane pyrimidine dimers (CPDs) and pyrimidine (6-4) pyrimidone photoproducts ((6-4)PPs), the Dewar photoproducts (DewarPPs), the valence isomer of (6-4)PPs (see Figure 1), have received much less attention to date. In 1964, it was first observed by Johns et al.[3] and found to be neither quantitatively nor biologically negligible in solar cytotox-ictiy and mutagenesis.[4]

The photolyase is a flavoprotein which uses UV light energy to split the photodamaged lesions via the electron-transfer redox cycle of the flavin molecules in organisms.[5] There are plenty of studies concerning the enzymatic repair pathways of CPDs and (6-4)PPs.[5−19] Among those, an oxetane intermediate involved in the repair mechanism of (6-4)PPs was often suggested by both theoretical and experimental studies.[10−13] Nonetheless, it was questioned by Domratcheva and Schlichting, who proposed a nonoxetane repair mechanism.[14]

In addition, taking the protein environment into consideration, there are different hypothetical repair mechanisms in relation to two conserved histidine residues.[15−19] These two conserved histidines, which are His365 and His369 in Figure 1, were proposed to play a pivotal role for the DNA repair

activity.[15,18,19] First, these histidines' different protonation states may markedly influence the pH of the active site, and it was observed that the (6-4) photolyase exhibits significant pH-dependent changes for repair activity in vitro.[19] Moreover, these two highly conserved histidines were suggested to catalyze the formation of the oxetane intermediate[15] or the transient-water-molecule-formation model[16,17] from the (6-4) photopro-duct. A recent ENDOR study[19] and ultrafast spectroscopy[18] revealed that the histidine close to the ribityl chain of the FAD (His365 in Figure 1) is likely protonated and the proton transfer between this histidine and (6-4)PP is an essential step in catalysis. A former interpretation of different experimental observations requires detailed work about the role of these two histidines and different protonation states of His365.

Similar to CPDs and (6-4)PPs, DewarPPs can be repaired by photolyases. However, due to the low yield and difficulties in detection, the photoreactivity and repair mechanism of DewarPPs has not yet been well-understood to date. Very recently, Glas et al. reported that the repair of DewarPPs by (6-4) photolyase involved a rearrangement of the Dewar lesions into the corre-sponding (6-4)PPs via direct C−N bond cleavage,[20] which requires electron injection from the singlet excited state of

FADH$^-$. Our previous work showed that the isomerization from T(dew)T to T(6-4)T in the neutral ground state has a very high barrier (about 30 kcal/mol), while it is sharply reduced to 15 kcal/mol when one electron is injected.[21]

In the current study, several enzymatic repair pathways are studied by the density functional theory method. From our calculations, the rearrangement of the Dewar lesions into the corresponding (6-4) lesions with electron injection was validated as the most efficient repair pathway. The role of the two conserved histidines has also been examined. These results contribute to the detailed understanding of the repair mechanism of DNA photolesions.

2. COMPUTATIONAL DETAILS

A model of the active site is designed based on the crystal structure of (6-4) photolyase in complex with DewarPP T(dew)C (PDB code: 2WQ6[20]). As shown in Figure 1, the model includes the His365-His369-Tyr423 triad which is believed to be important for catalysis,[22] the flavin adenine nucleotide (FAD) cofactor (simplified by its adenine part), and the 2′-OH group, as well as residue Q299 due to the strong hydrogen bonds formed with the lesion. We particularly consider His365 as both neutral (HIE) and protonated (HIP) options in our active site model to investigate the influence of the different
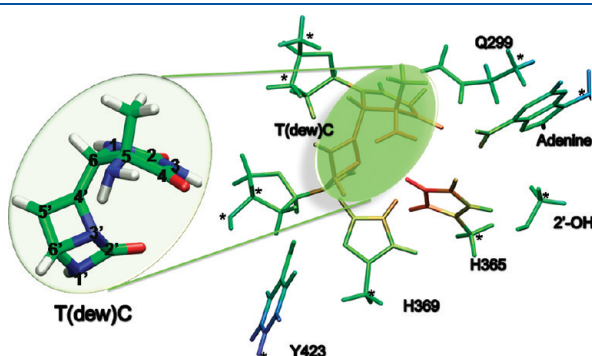

Figure 1. Structure of the T(dew)C photoproduct (left) and the active site in (6-4) photolyase (right). PDB code: 2WQ6.

protonation states. The truncation atoms were fixed to their X-ray positions to keep the optimized geometries close to the experimental ones and labeled with asterisks. Apart from these centers, the geometries were fully optimized, including those of transition states.

The repair of the T(dew)C involves not only the transfer of the amino group to the C4′ atom but also a N3′−C6′ bond breaking process which causes the isomerization from T(dew)C to T(6-4)C. Former C−N breaking (NH$_2$ transfer) pathways are noted as A, B, and C pathways in this paper. The transition state of the later N3′−C6′ bond breaking process is noted as TS-RA. In this paper, we propose that the electron donation from the flavin cofactor occurs directly into the DewarPP, forming the radical anion. Therefore, the calculations are in the radical anionic ground state if there is no special instruction.

A standard procedure in the cluster approach for modeling enzymes is used in this work.[23,24] This approach has been systematically assessed and successfully applied to a large number of enzymes.[25−27] The B3LYP hybrid functional was used in the present work. The standard 6-31G(d) basis set was used throughout the geometry optimizations. To obtain more accurate energies, the larger 6-311++G(2d,2p) basis set was employed to perform single-point calculations based on the optimized structures. Frequency calculations were performed to confirm the nature of stationary points and transition states. The locking procedure leads to several small imaginary frequencies, typically below 40i cm^{-1}. These contribute insignificantly to the ZPE and can be ignored.[23,24] To consider the solvation effects from the surrounding protein, single-point calculations were carried out with a polarizable continuum model (IEF-PCM).[28−30] The dielectric constant of 4 was used to model the parts of the enzyme that are not included in the quantum chemical active site model.[23−25] All calculations were performed using the Gaussian 03 software package.[31]

3. RESULTS AND DISCUSSION

3.1. Repair Mechanisms for Neutral Histidine HIE365. First, we consider the His365 in its neutral state HIE365 in our active site model (with 127 atoms in total). The optimized geometries
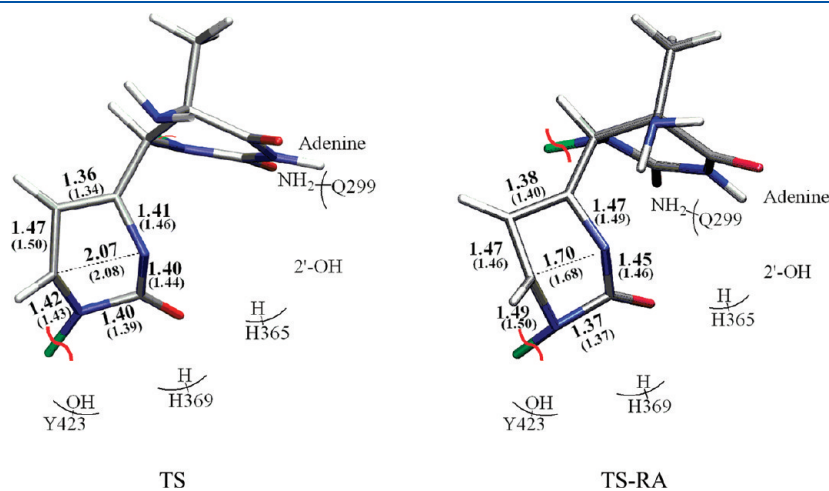

Figure 2. Optimized transition state structures for the N3′−C6′ bond cleavage for the neutral (TS) and radical anion (TS-RA) molecules in the photolyase. Geometrical parameters with HIE 365 and HIP365 (in parentheses) are labeled at the UB3LYP/6-31G(d) level.
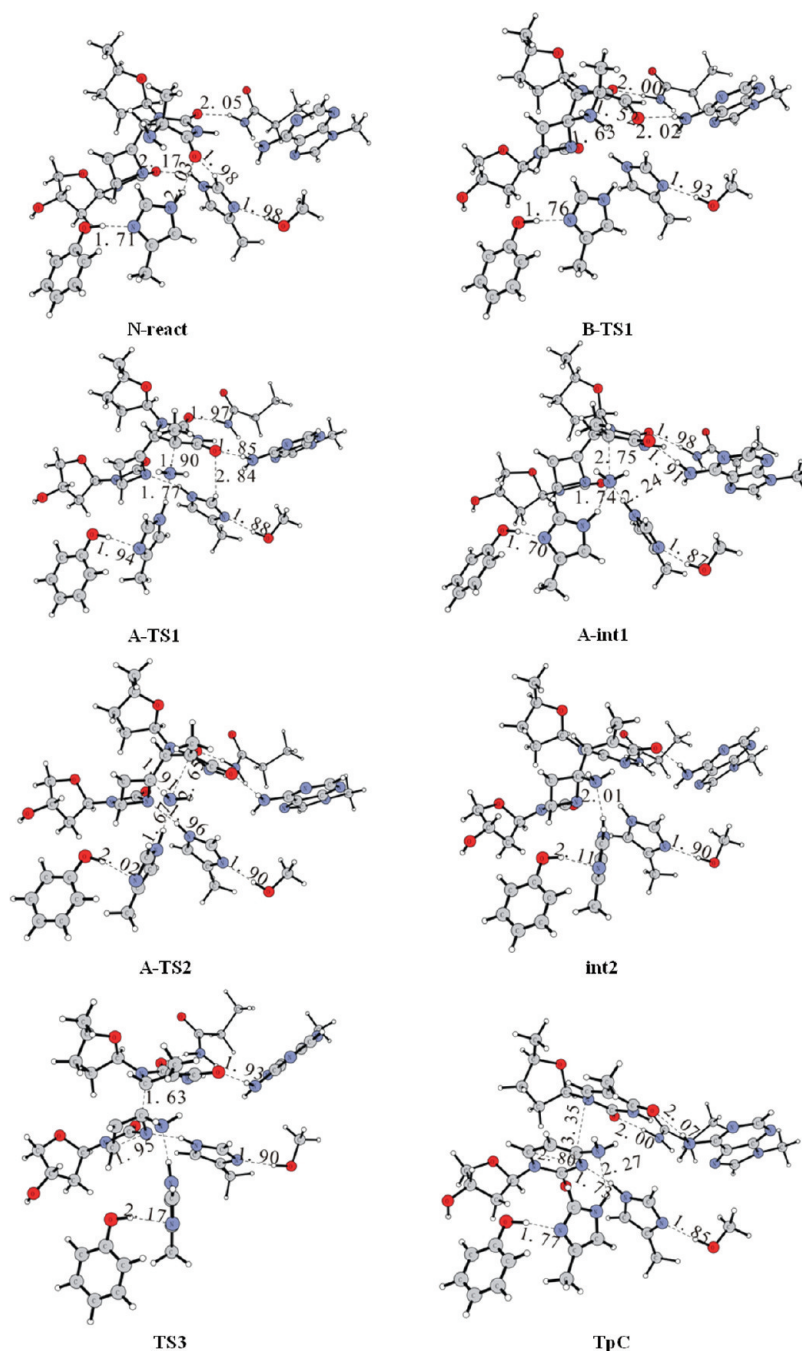
Figure 3. Optimized structures of the transition states and intermediates along the reaction pathway for substrate orientation A and B with the HIE365 model.

for all stationary points are depicted in Figures 2 and 3, and energy profiles are summarized in Figure 4.

In N-react which is the reactant of the neutral (N) HIE365 model, the DewarPP lesion is stabilized by two histidines and surrounding hydrogen bonding networks. For His369, the hydrogen bond between NA-H and O4 is 2.03 Å, and His369 establishes another strong hydrogen bond of 1.71 Å with the OH group of Tyr423. HIE365 forms three hydrogen bonds with O4 of Dewar PP (1.98 Å), O2′ of Dewar PP (2.17 Å), and 2′-hydroxyl of FAD (1.98 Å), respectively. A hydrogen bond is also found between O2 of DewarPP and Gln299 (2.05 Å). The vertical electron affinity (EA) for N-react is −6.4 kcal/mol, and

the adiabatic EA is 9.3 kcal/mol. So the reaction is exothermic when accepting an electron.

The optimized structure of transition state (TS) for the N3′−C6′ bond cleavage in the radical anion form, TS-RA, is shown in Figure 2. The N3′−C6′ distance is 2.07 Å in neutral TS, while it is much shorter (1.70 Å) in TS-RA. The electron in radical anion is delocalized over C4′, C5′, and C6′ of dewar part and C4 of pyrimidine ring. Recent experimental data[20] presented that the repair of Dewar isomers by (6-4) photolyase involved electron injection process with the rearrangement of the Dewar lesions into the corresponding (6-4) lesions. Our previous calculations[21] on T(dew)T model has revealed that,
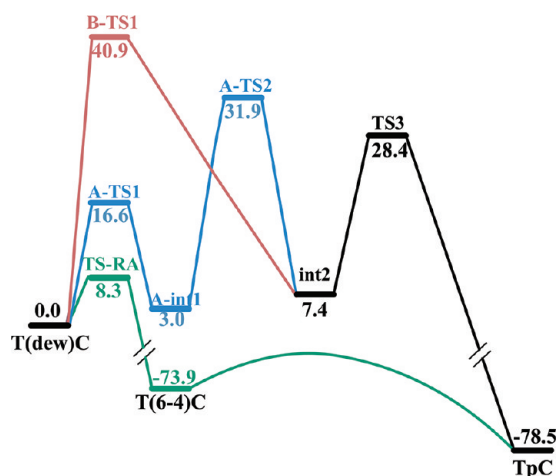
Figure 4. Calculated potential energy profiles (energies in kcal/mol) in three different orientations for the HIE365 model.

Table 1. Calculated Relative Energies for the 6-4PP and DewarPP in the Ground State via Neutral and Radical Anion (RA) Pathway at the PCM/B3LYP or UB3LYP/6-311++G-(2d,2p) Level

TpC	relative energy (kcal/mol)	
	HIE365	HIP365
T(6-4)C	0.00	0.00
TS	86.47	74.50
T(dew)C	56.27	41.63
T(6-4)C-(RA)	0.00	0.00
TS-RA	82.24	80.02
T(dew)C-(RA)	73.92	74.98

if one electron was injected to form radical anion, the barrier of the isomerization from DewarPP into (6-4)PP was sharply decreased. Similar to T(dew)T,[21] the dissociation of the N3′-C6′ bond in the singlet neutral pathway requires almost 30 kcal/mol activation energy, while it only needs 8.3 kcal/mol in HIE365 model through the radical anion structure; see Table 1.

Why are isomerization reactions of anion radical much faster than neutral one? The cleavage of the thymine photodimer of anion radical has a much lower barrier than the neutral one which resists decomposition even at above 200 °C.[32] Shaik and Shurki used the VB diagram to appreciate this effect. The cycloaddition of the anion radical requires the promotion of the only π-bond (singlet−triplet excitation), while the promotion of both π-bonds are needed for the neutral case. The barrier is directly proportional to the total promotion energy, and therefore, the barrier for the radical anion case is much lower.[33] Therefore, when one electron is injected, in addition to electrostatic interactions, the essential decrease of the promotion energy speeds up the isomerization reaction and results in a significant drop in its barrier. Such a low barrier of this N3′−C6′ cleavage reaction indicates effective isomerization of the DewarPP with electron injection has a competitive advantage in the repair mechanism.

Next, we studied the amino group transfer pathways. For the amino group transfer, three possible orientations can be envisioned; see Scheme 1. In pathway A and C, the amino group transfer is stepwise, in which the leaving NH_2^- is stabilized through a hydrogen bond to one of the two histidines (path A: his369, path C: his365) via transition state TS1. Then it goes through TS2 to attack the C4′ and finally finish the transfer process. In pathway B, the amino group transfer is concerted without the involvement of two histidines. If we look carefully at the structure of N-react, His369 sits on the more preferred position than HIE365 for accepting the transferred amino group. So when the amino group leaves the lesion molecule, it may attach to His369, which is called pathway A here. We optimized the transition state for the C−N bond cleavage (A-TS1) and the resulting intermediate (A-Int1), which are shown in Figure 3. The C−N bond cleavage barrier is found to be 16.6 kcal/mol, which is 8.3 kcal/mol higher than that of TS-RA. The C−N distance is 1.90 Å of A-TS1 and increases to

2.75 Å in A-Int1. On the contrary, the N−NA−H distance decreased from 2.03 Å in HIE-react to 1.77 Å in A-TS1 and 1.74 Å at A-Int1. This clearly implies that His369 stabilizes the transferred amino group and resulted in a stable intermediate. The following step is the nucleophilic attack of amino group (NH_2) on the C4′ of DewarPP. We also find the transition state A-TS2 and the final product int2 as shown in Figure 3. The C4′−N distance is located at 1.91 Å, and the calculated barrier is 28.9 kcal/mol. It is interesting to see that the hydrogen bond between the His369 and the NH_2 group becomes stronger at A-TS2 but weaker at A-int2. The His369 provides again stabilization to the transition state with the hydrogen bond. An additional transition state TS3 (C−N bond cleavage involved) is needed to split the two regular bases. On the whole, the high barriers for this pathway A rule out this mechanistic possibility.

Pathway B does not involve the participation of the two conserved histidines. The optimized structure of the transition state B-TS1 is displayed in Figure 3. The direct amino group transfer in DewarPP results in a four-membered ring structure. The corresponding C−N distances in B-TS1 are 1.52 Å and 1.63 Å, respectively. The four-membered ring is highly strained with relatively high energy. The calculated reaction barrier for this concerted pathway is 40.9 kcal/mol, which makes pathway B an unlikely mechanistic option.
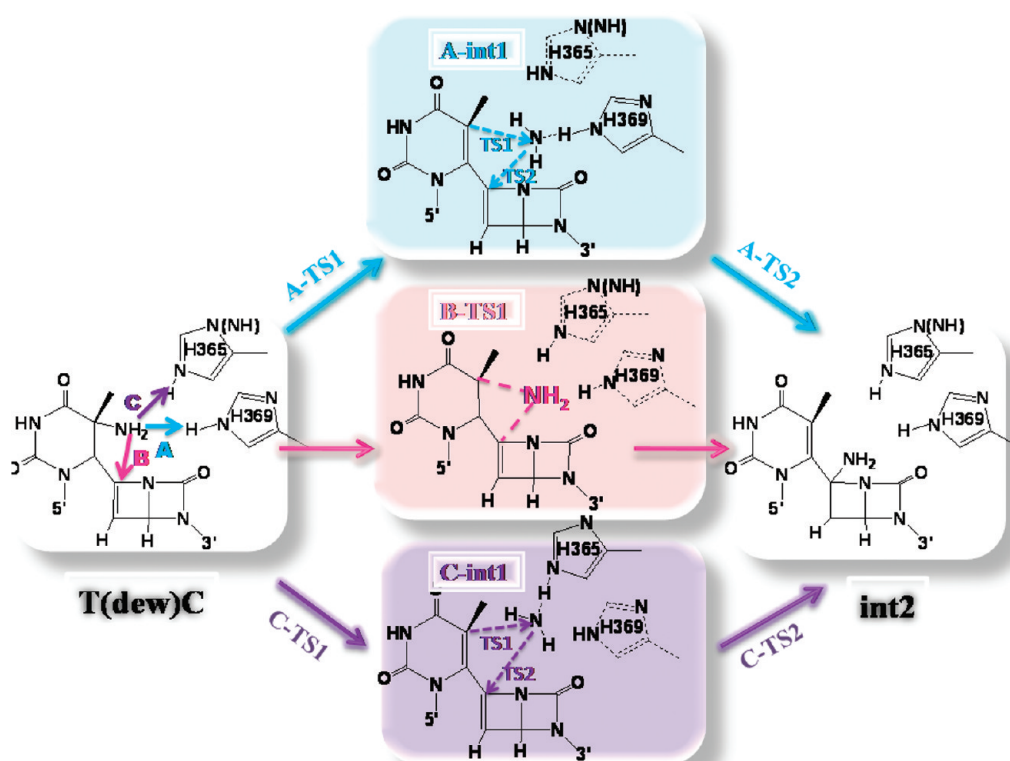
For pathway C, due to the strong hydrogen bonding between NH_2 group and His369, every attempt to locate a transition state leads to A-TS1.

In summary, compared with an isomerization reaction, other possible repair channels in T(dew)C have relatively much higher barriers. If one electron is injected into T(dew)C lesion, the N3′−C6′ bond breaking will take place fast ahead of other possible pathways.

3.2. Repair Mechanisms for Protonated Histidine HIP365. In this part, we consider His365 as protonated HIP residue, and the model is 128 atoms. We summarized the optimized geometries and the potential energy profiles in Figures 5 and 6, respectively. Those main hydrogen-bonding networks are retained in the reactant of the protonated HIP365 model (P-react). Different from N-react, the central HIP365 forms hydrogen bond with N3′ of DewarPP instead of O2′. Meanwhile, there is a strong hydrogen bond between adenine group and O4 of lesion. The vertical electron affinity (EA) for P-react is 44.6 kcal/mol, while the adiabatic EA is 56.7 kcal/mol. Compared with the N-react, the large EA values for P-react indicate that the electron injection is much more energetically feasible when the His365 is protonated.

10979

dx.doi.org/10.1021/jp204128k |*J. Phys. Chem. B* 2011, 115, 10976−10982

Scheme 1. Three Possible Reaction Mechanisms for the Repair of T(dew)C TS TS-RA

The summarized structural parameters and energies are listed in Figure 2 and Table 1, respectively. For the neutral molecule, the transition state of the N3′−C6′ cleavage is 30.0 kcal/mol higher than the reactant, and the N3′−C6′ bond distance is 2.08 Å. The C−N distance decreases to 1.68 Å of TS-RA with the barrier of only 5.0 kcal/mol. The spin densities for TS-RA are also delocalized over C4, C4′, C5′, and C6′ of the dewar ring. The isomerization barrier of the protonated His365 is about 3 kcal/mol lower than that in neutral one.

We also studied the amino group transfer mechanism in orientation A in a similar fashion as for the HIE365 process, which is depicted in Figure 6. The barrier is calculated to be 17.4 kcal/mol relative to the P-react, which is quite close to that in the HIE365 case. In this situation, His369 provides stabilization on the TS and intermediate through hydrogen bonds. Since His365 is protonated, it can deliver a proton to (6-4)PP lesion (pathway C), which was assumed to be the key step of the repair photocycle.[18] We located the transition state of the proton transfer from HIP365 to teh NH_2 group (P-C-TS1). The proton resides in the middle of two nitrogen atoms. The proton transfer produces a neutral NH_3 molecule in intermediate P-C-int1. The proton transfer takes place easily with a barrier of only 5.8 kcal/mol of barrier. For the following C−N cleavage step, the transition state P-C-TS2 is located at C−N distance of 1.64 Å, and it is 4 kcal/mol higher than P-C-int2. The low barrier proposes that the formation of NH_3 facilitates the direct breakage of the C−N bond at the 5′ base. After releasing the NH_3 group, we found a very stable intermediate P-C-int2 which is 23.9 kcal/mol lower than reactant. The C−N distance is 3.88 Å then. Although the following transition state for nucleophilic attack, P-C-TS3, is just 25.2 kcal/mol higher

above the reactant, owing to the stability of P-C-int2, the repair process through orientation C can never happen without enough energy. The protonated His365 results in geometrical changes of the protein environment and opens a new repairway via proton transfer. However, the proton transfer mechanism still cannot compete with the fast isomerization between T(dew)C and T(6-4)C. Because of the electrostatic repulsion from the protonated HIP365, the concerted amino group transfer intermediate has even high energy, which will not be presented here.

In our work, we showed that His365 and His369, which are close to the DewarPP lesion and flavin cofactor, play a critical role in enzymatic DNA repair. For T(dew)C, the key amino group transfer process takes place with a lower barrier under the help of conserved His369, which forms a strong hydrogen bond with the NH_2 group. Furthermore, the change in the protonation state of His365 causes small but important reorientations of the protein side chains and makes the HIP365 face the NH_2 group. Then proton transfer from HIP365 to NH_2 occurs fast with a very low reaction barrier. However, the following nucleophilic attack to the C4′ of the 3′ base has a relatively high barrier to pass in both situations.

Compared with above amino group transfer repair mechanisms, the direct N3′−C6′ bond cleavage of isomerization from T(dew)C to T(6-4)C is the most efficient one. It is worth to mention that a previous study showed the different Dewar PPs possessing a distinct repair efficiency in (6-4) photolyase.[34] We can conclude that the different activation energy needed for T(dew)T (15.4 kcal/mol)[21] and T(dew)C (8.3 kcal/mol) seems to be the most important factor for the different repair efficiencies of these two Dewar PPs.
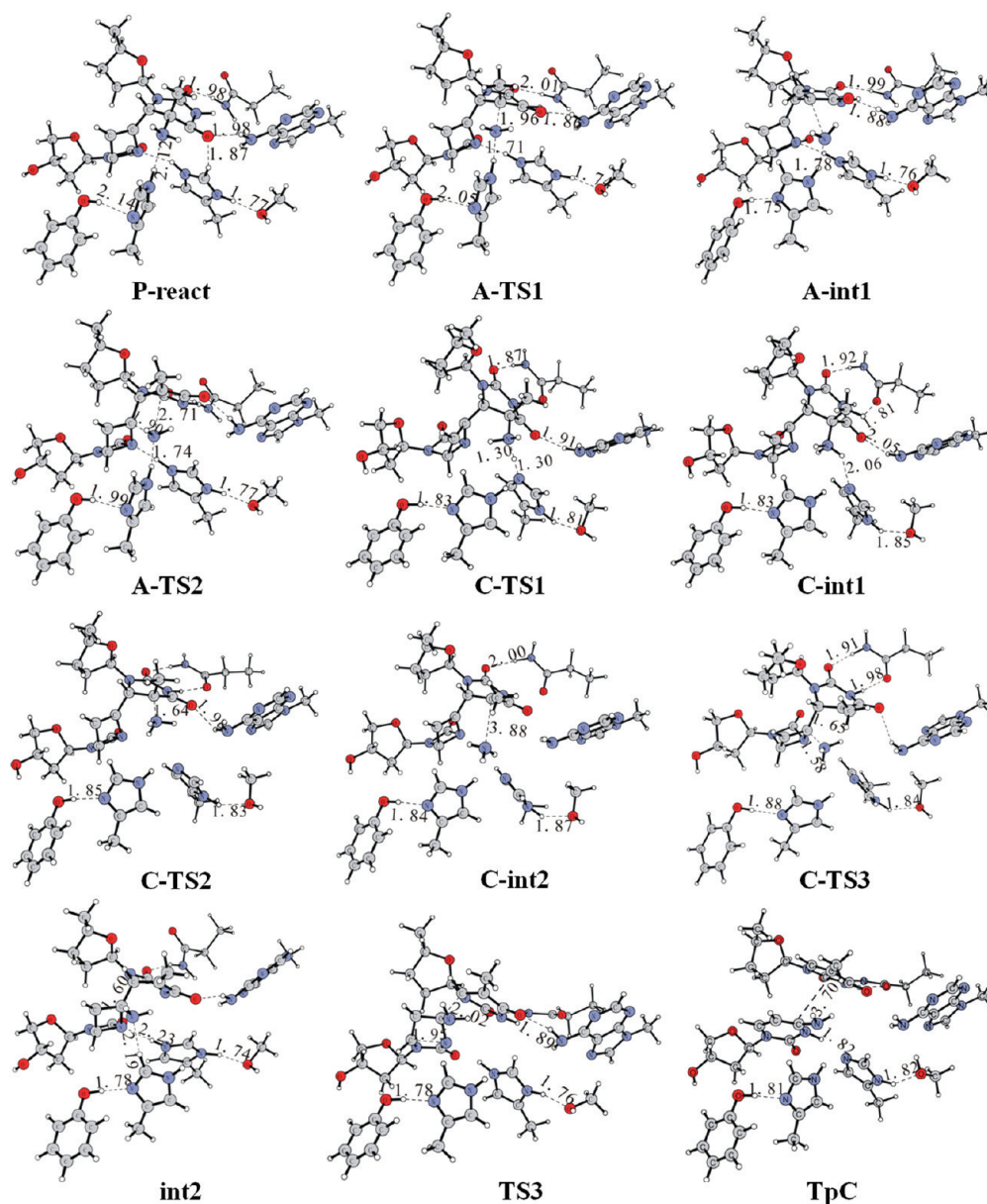
Figure 5. Optimized structures of the transition states and intermediates along the reaction pathway for substrate orientation A and C with the HIP365 model.
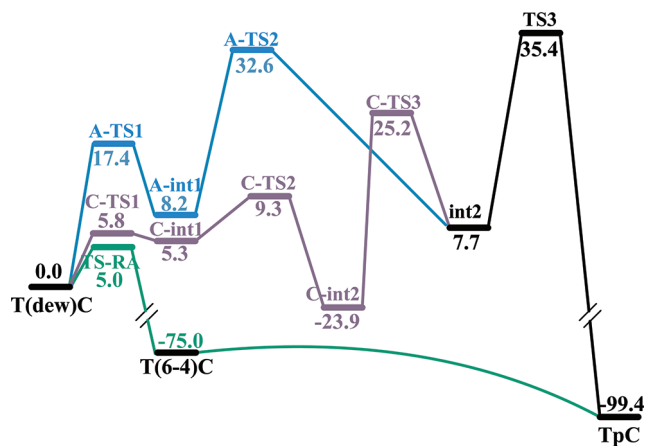

Figure 6. Calculated potential energy profiles (energies in kcal/mol) in different orientations for the protonated His365.

4. CONCLUSION

In this work, the repair mechanism of DNA Dewar photoproduct T(dew)C in (6-4) photolyase is studied by using hybrid density functional theory. Both neutral and protonated His were considered, and the roles of two reserved histidines in the mechanism of repair of the Dewar lesions by (6-4) DNA photolyases have also been discussed. We found that residue His369 can stabilize both the intermediate and the transition states. The protonated His365 makes changes of the protein environment and opens a new repairway via proton transfer. The isomerization from DewarPP into (6-4)PP with one electron injection is energetically very favorable. Three plausible amino group transfer pathways were investigated but turned out to have much higher barriers. On the basis of these findings, we propose that the catalytic cycle for the repair of DewarPP needs corresponding isomerization to (6-4)PP, which supports the hypothesis by the experimentalist.[20]

10981

dx.doi.org/10.1021/jp204128k |*J. Phys. Chem. B* 2011, 115, 10976–10982

■ REFERENCES

(1) Pfeifer, G. P.; You, Y.-H.; Besaratinia, A. Mutations induced by ultraviolet light. *Mutat. Res.* **2005**, *571*, 19–31.

(2) Taylor, J. S. *Acc. Chem. Res.* **1994**, *27*, 76–82.

(3) Johns, H. E.; Pearson, M. L.; LeBlanc, J. C.; Helleiner, C. W. *J. Mol. Biol.* **1964**, *9*, 503–524.

(4) Perdiz, D.; Grof, P.; Mezzina, M.; Nikaido, O.; Moustacchi, E.; Sage, E. *J. Biol. Chem.* **2000**, *275*, 26732–26742.

(5) Sancar, A. *Chem. Rev.* **2003**, *103*, 2203–2237.

(6) Zhong, D. *Curr. Opin. Chem. Biol.* **2007**, *11*, 174–181.

(7) Asgatay, S.; Petermann, C.; Harakat, D.; Guillaume, D.; Taylor, J. S.; Clivio, P. *J. Am. Chem. Soc.* **2008**, *130*, 12618–12619.

(8) Kwok, W. M.; Ma, C.; Phillips, D. L. A doorway state leads to photostability or triplet photodamage in thymine DNA. *J. Am. Chem. Soc.* **2008**, *130*, 5131–5139.

(9) Durbeej, B.; Eriksson, L. A. Reaction mechanism of thymine dimer formation in DNA induced by UV light. *J. Photochem. Photobiol., A* **2002**, *152*, 95–101.

(10) Zhao, X.; Liu, J.; Hsu, D. S.; Zhao, S.; Taylor, J. S.; Sancar, A. *J. Biol. Chem.* **1997**, *272*, 32580–32590.

(11) Kim, S. T.; Malhotra, K.; Smith, C. A.; Taylor, J. S.; Sancar, A. *J. Biol. Chem.* **1994**, *269*, 8535–8540.

(12) Heelis, P. F.; Liu, S. *J. Am. Chem. Soc.* **1997**, *119*, 2936–2937.

(13) Sadeghian, K.; Bocola, M.; Merz, T.; Schütz, M. *J. Am. Chem. Soc.* **2010**, *132*, 16285–16295.

(14) Domratcheva, T.; Schlichting, I. *J. Am. Chem. Soc.* **2009**, *131*, 17793–17799.

(15) Hitomi, K.; Nakamura, H.; Kim, S. T.; Mizukoshi, T.; Ishikawa, T.; Iwai, S.; Todo, T. *J. Biol. Chem.* **2001**, *276*, 10103–10109.

(16) Maul, M. J.; Barends, T. R.; Glas, A. F.; Cryle, M. J.; Domratcheva, T.; Schneider, S.; Schlichting, I.; Carell, T. *Angew. Chem., Int. Ed. Engl.* **2008**, *47*, 10076–10080.

(17) Glas, A. F.; Schneider, S.; Maul, M. J.; Hennecke, U.; Carell, T. *Chem.—Eur. J.* **2009**, *15*, 10387–10396.

(18) Li, J.; Liu, Z. Y.; Tan, C. T.; Guo, X. M.; Wang, L. J.; Sancar, A.; Zhong, D. P. *Nature* **2010**, *466*, 887–890.

(19) Schleicher, E.; Hitomi, K.; Kay, C. W.; Getzoff, E. D.; Todo, T.; Weber, S. *J. Biol. Chem.* **2007**, *282*, 4738–4747.

(20) Glas, A. F.; Kaya, E.; Schneider, S.; Heil, K.; Fazio, D.; Maul, M. J.; Carell, T. *J. Am. Chem. Soc.* **2010**, *132*, 3254–3255.

(21) Ai, Y. J.; Liao, R. Z.; Chen, S. F.; Luo, Y.; Fang, W. H. *J. Phys. Chem. B* **2010**, *114*, 14096–14102.

(22) Maul, M. J.; Barends, T. R.; Glas, A. F.; Cryle, M. J.; Domratcheva, T.; Schneider, S.; Schlichting, I.; Carell, T. *Angew. Chem., Int. Ed.* **2008**, *47*, 10076–10080.

(23) Himo, F. *Theor. Chem. Acc.* **2006**, *116*, 232–240.

(24) Siegbahn, P. E. M.; Himo, F. *J. Biol. Inorg. Chem.* **2009**, *14*, 643–651.

(25) (a) Himo, F.; Siegbahn, P. E. M. *Chem. Rev.* **2003**, *103*, 2421–2456. (b) Noodleman, L.; Lovell, T.; Han, W.-G.; Li, J.; Himo, F. *Chem. Rev.* **2004**, *104*, 459–508. (c) Siegbahn, P. E. M.; Borowski, T. *Acc. Chem. Res.* **2006**, *39*, 729–738.

(26) (a) Chen, S.-L.; Pelmenschikov, V.; Blomberg, M. R. A.; Siegbahn, P. E. M. *J. Am. Chem. Soc.* **2009**, *131*, 9912–9913. (b) Chen, S.-L.; Blomberg, M. R. A.; Siegbahn, P. E. M. *J. Phys. Chem. B* **2011**, *115*, 4066–4077. (c) Chen, S.-L.; Fang, W.-H.; Himo, F. *J. Phys. Chem. B* **2007**, *111*, 1253–1255.

(27) (a) Liao, R.-Z.; Yu, J.-G.; Himo, F. *J. Chem. Theory Comput.* **2011**, *7*, 1494–1501. (b) Liao, R.-Z.; Yu, J.-G.; Himo, F. *J. Phys. Chem. B* **2010**, *114*, 2533–2540. (c) Liao, R.-Z.; Yu, J.-G.; Himo, F. *Proc. Natl. Acad. Sci. U.S.A.* **2010**, *107*, 22523–22527.

(28) Cossi, M.; Scalmani, G.; Rega, N.; Barone, V. *J. Chem. Phys.* **2002**, *117*, 43–54.

(29) Cossi, M.; Rega, N.; Scalmani, G.; Barone, V. *J. Comput. Chem.* **2003**, *24*, 669–681.

(30) Cossi, M.; Barone, V.; Robb, M. A. *J. Chem. Phys.* **1999**, *111*, 5295–5302.

(31) Frisch, M. J.; Trucks, G. W.; Schlegel, H. B.; Scuseria, G. E.; Robb, M. A.; Cheeseman, J. R.; Montgomery, J. A., Jr.; Vreven, T.; Kudin, K. N.; Burant, J. C.; Millam, J. M.; Iyengar, S. S.; Tomasi, J.; Barone, V.; Mennucci, B.; Cossi, M.; Scalmani, G.; Rega, N.; Petersson, G. A.; Nakatsuji, H.; Hada, M.; Ehara, M.; Toyota, K.; Fukuda, R.; Hasegawa, J.; Ishida, M.; Nakajima, T.; Honda, Y.; Kitao, O.; Nakai, H.; Klene, M.; Li, X.; Knox, J. E.; Hratchian, H. P.; Cross, J. B.; Adamo, C.; Jaramillo, J.; Gomperts, R.; Stratmann, R. E.; Yazyev, O.; Austin, A. J.; Cammi, R.; Pomelli, C.; Ochterski, J. W.; Ayala, P. Y.; Morokuma, K.; Voth, G. A.; Salvador, P.; Dannenberg, J. J.; Zakrzewski, V. G.; Dapprich, S.; Daniels, A. D.; Strain, M. C.; Farkas, O.; Malick, D. K.; Rabuck, A. D.; Raghavachari, K.; Foresman, J. B.; Ortiz, J. V.; Cui, Q.; Baboul, A. G.; Clifford, S.; Cioslowski, J.; Stefanov, B. B.; Liu, G.; Liashenko, A.; Piskorz, P.; Komaromi, I.; Martin, R. L.; Fox, D. J.; Keith, T.; Al-Laham, M. A.; Peng, C. Y.; Nanayakkara, A.; Challacombe, M.; Gill, P. M. W.; Johnson, B.; Chen, W.; Wong, M. W.; Gonzalez, C.; Pople, J. A. *Gaussian 03*, revision C.02; Gaussian, Inc.: Pittsburgh, PA, 2004.

(32) Begley, T. P. *Acc. Chem. Res.* **1994**, *27*, 394–401.

(33) Shaik, S.; Shurki, A. *Angew. Chem., Int. Ed.* **1999**, *38*, 586–625.

(34) Glas, A. F.; Schneider, S.; Maul, M. J.; Hennecke, U.; Carell, T. *Chem.—Eur. J.* **2009**, *15*, 10387–10396.

10982

dx.doi.org/10.1021/jp204128k |*J. Phys. Chem. B* 2011, 115, 10976–10982